Artillery Shell Drift at High Angles of Fire

W. Z. Collings* and R. F. Lieske†
U.S. Army Ballistic Research Laboratories, Aberdeen Proving Ground, Md.

Spin-stabilized projectiles were instrumented with yawsondes and fired at various launch angles to obtain information on the phenomenon of left drift. The measuring system and data reduction procedures are discussed. At low launch angles, projectiles drift to the right of the line of fire with a normal nose forward orientation. At high angles of launch and low velocities, projectiles fly base forward during descent and drift to the left of the line of fire. Small yaw aerodynamic coefficients are obtained from the yawsonde data using a numerical integration method. Six-degree-of-freedom simulations compare favorably with flight observations.

Nomenclature

C_{l_p} = roll moment/$(\frac{1}{2})\rho V^2 Sd(pd/V)$ negative coefficient: moment decreases roll rate, p
$C_{M_{p\alpha}}$ = Magnus moment/$(\frac{1}{2})\rho V^2 Sd(pd/V)\delta$ positive coefficient: moment rotates nose ∠ plane of α_t in direction of spin
$C_{M_q} + C_{M_{\dot\alpha}}$ = damping moment/$(\frac{1}{2})\rho V^2 Sd(q_t d/V)$ positive coefficient: moment increases angular velocity
C_{M_α} = static moment/$(\frac{1}{2})\rho V^2 Sd\delta$ positive coefficient: moment increases angle of attack α_t; $\delta = \sin\alpha_t$
d = body diameter of projectile, reference length
p = roll rate
q,r = transverse angular velocities
q_t = $(q^2+r^2)^{\frac{1}{2}}$
QE = quadrant elevation
S = $(\pi d^2/4)$, reference area
t = time of flight
V = velocity of projectile
x = interval between successive sun sensor pulses
y = interval between alternate sun sensor plates
ρ = air density
σ_N = solar aspect angle (angle between normal to longitudinal axis of shell and solar vector)

I. Introduction

THE yaw of respose is the steady-state angle of attack due to gravity-induced curvature of the trajectory.[1] Theory predicts that a projectile with positive (right-hand) spin will trim at this equilibrium angle such that its nose is to the right of the flight path. Associated with this trim angle is a lift force which causes the projectile to drift to the right of the line of fire. Observations have confirmed right deflection and it has been generally accepted that all spin-stabilized projectiles deflect to the right. Indeed, corrections for right deflections are incorporated in the firing tables for each artillery system.

Range data and field reports, however, show that artillery shell when fired in the "minimum range-maximum quadrant elevation" mode, i.e., at low velocities and high angles, exhibit erratic flight and frequently impact to the left of the line of fire.[2] For example, Fig. 1 shows quadrant elevation vs deflection at impact for the 105mm M1 shell fired at a nominal muzzle velocity of 205 m/sec. Positive deflection indicates deflection to the right of the line of fire. For quadrant elevations less than 70°, the deflection increases to the right with increasing quadrant elevation. At 75° and above, however, there is drift reversal with left deflections up to 200 m.

Such observations led to a more thorough and systematic program for studying the motion of profectiles fired at high quadrant elevations and low velocities. Information on the system of aerodynamic forces and moments which causes a change in the direction of the drift is of importance. Presented here are the results and analysis of a range firing program using projectiles instrumented with solar aspect sensors. The measuring system and data reduction procedures are briefly described. Efforts to extract aerodynamic coefficients from the data are included. Simulated solar aspect angle histories, based on the six-degree-of-freedom trajectory model, are compared with flight observations.

II. Measurement System

The solar aspect angle, σ_N, is the angle between a normal to the longitudinal axis of the projectile and a vector directed from the center of mass to the sun (see Fig. 2). Solar aspect sensors, commonly called yawsondes, measure this angle as a function of time of flight. The *BRL* yawsonde consists of two sun sensors (photovoltaic cells) mounted behind slits which are about 180° apart on the surface of the projectile. The two slits, each at an angle with respect to the longitudinal axis,

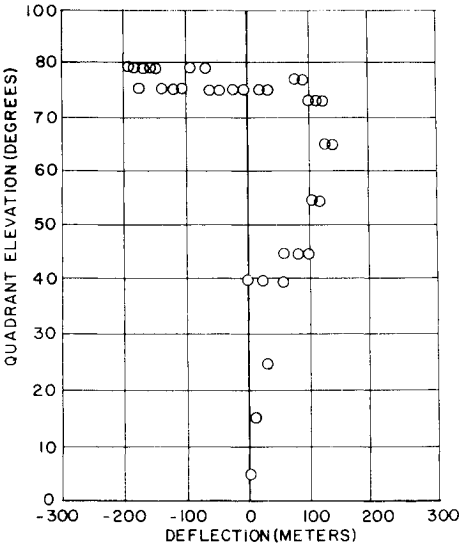

Fig. 1 Quadrant elevation vs deflection for the 105mm M1 shell; nominal muzzle velocity: 205 m/sec.

Received June 7, 1974; revision received October 24, 1974.
Index categories: LV/M Trajectories; LV/M Simulation; LV/M Flight Testing.

*Mechanical Engineer, Free Flight Aerodynamics Branch, Exterior Ballistics Laboratory. Member AIAA.
†Chief, Flight Simulation Section, Firing Tables Branch, Exterior Ballistics Laboratory. Member AIAA.

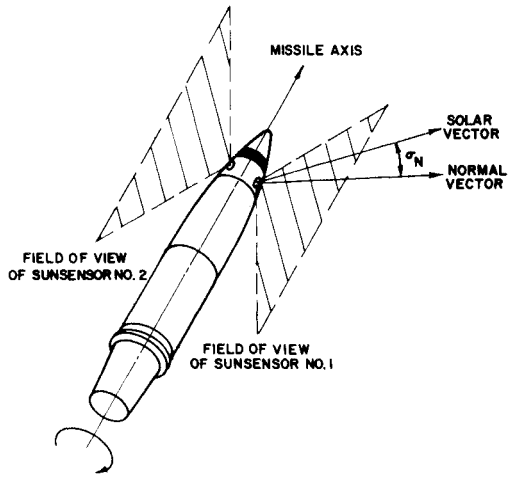

Fig. 2 Sensor fields of view and solar aspect angle.

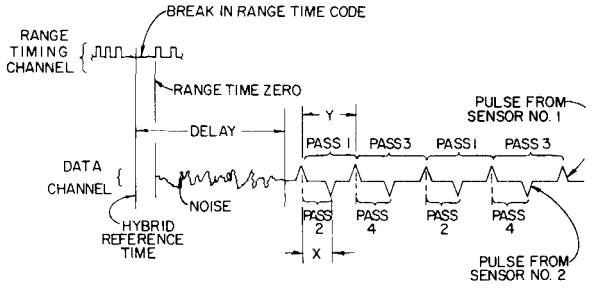

Fig. 3 Data pulse train illustrating the four-pass method of reduction.

define two narrow fields of view in space. As the projectile rolls, the solar vector alternately intercepts the fields of view of the two sensors, and electrical pulses are produced. The solar aspect angle is related through calibration to the phase relationship between the pulses from the two sensors. The phase relationship between the pulses from the two sensors will change as the projectile pitches and yaws in flight. The period of the rolling motion is the time between successive intercepts of the same field of view with the solar vector. Thus, the spin history is obtained also. The pulse data, therefore, are a measure of the in-flight motion of the projectile. The calibration procedure[3] gives aspect angle vs x/y, where x and y are defined in Fig. 3. According to convention, the aspect angle is positive if the solar vector lies between the normal and the nose of the projectile. The calibration can resolve 15 sec of arc in σ_N and is repeatable to within 0.1°. The coefficients in a calibration equation for aspect angle as a function of x/y are obtained by the least squares technique.

The yawsonde data are transmitted from projectile to ground by an FM/FM telemetry system. See Ref. 4 and 5 for details. The ground station is a system of high gain antennas, FM receivers, and magnetic tape recorders. Range time is recorded simultaneously with the yawsonde data. Projectile trajectory data are provided by an FPS-16 tracking radar which measures range to within ± 4.6 meters (rms) and to within ± 0.1 mil (rms). Meteorological data are also taken.

III. Reduction of Yawsonde Data

A data sample is a three-pulse ensemble as shown in Fig. 3. Since the frequency of the pulses is the roll rate of the projectile, the total number of samples during a flight is the product of the time of flight and the roll rate. For example, the 105mm flights described herein contain about 6000 data samples. With this large number of samples, automatic data handling is mandatory. Details of the automatic handling and reduction process can be found in Ref. 6.

The primary component in the data handling system is the EAI 690 Hybrid Computer. Supporting equipment consists of a magnetic tape system, a discriminator and signal-conditioning circuitry. The data channel is played back through the discriminator into the signal-conditioning circuit which compensates for bias in overall signal level and for asymmetries in pulse shape. The conditioned pulse train is the input for the analog section of the hybrid computer. The basic idea of the reduction method is to use the pulses to start and stop a sixteen bit digital timer. The required x/y data are simply the ratios of the timer periods.

The digital timer, driven by a 1-MHz internal clock, counts at a rate of one count every 2 μsecs. The maximum number of counts the timer can store is $2^{16} = 65536$ which is equivalent to approximately 130 msec. Hence, to recover all the data, it is necessary to play back the data more than once. Four separate passes at the data are taken in succession. Proper matching of the four passes is achieved by referencing the hybrid time to the break in the range timing code.

Immediately following launch, the signal is frequently noisy. Setting in a delay time insures that the hybrid computer has a reasonably clean pulse train to analyze. The time interval between the end of the delay and the first positive pulse is measured.

The calibration equation is applied to the measured x and y counts in the digital section of the hybrid computer. For preliminary examination of data, a high-speed printer output of solar aspect angle as a function of time is available. The time for a particular data sample is taken at the first pulse of the three-pulse ensemble, and running time is generated by the cumulative sum of passes one and three.

The output of the digital section is formatted on magnetic tape for later fitting with trajectory and astronomical data on a high-speed digital computer. Plots of solar aspect angle vs time are available from a digital plotter.

IV. Range Firing Program

The purpose of the program was to confirm left deflection and obtain quantitative trajectory and yawsonde data for projectiles fired at high launch elevations and low velocity. The 105-mm M1 artillery shell was selected for the firing program. This projectile has an overall length of approximately 49 cm with a 5-cm, 9° conical boattail and weighs 14.5 kg.

A total of eighteen projectiles were fired from a 105mm Howitzer tube at the NASA facility at Wallops Island, Va. Three shell were instrumented with yawsondes. The remaining fifteen were fired as calibration rounds. All shell were fired at a nominal muzzle velocity of 250 m/sec. The calibration rounds were fired at selected quadrant elevations to determine when left deflection occurs. When the onset of left deflection was established at a particular quadrant elevation, one yawsonde round was then fired at the same quadrant elevation. The firing program then called for an additional yawsonde round at an even higher quadrant elevation and presumably even further into the left drift region. The final yawsonde round was fired at an elevation just below that of onset so that the shell would experience normal right deflection.

The gun was on an azimuth of 130° clockwise from North. The optimum launch window occurs when the azimuthal plane of the gun is perpendicular to the sun's azimuthal plane. This condition was approximately in effect during the yawsonde flights.

V. Results

The shell were fired at launch angles between 70 and 82°. The maximum angle of fire in the firing tables for the 105mm shell is about 73°; and, at or below this angle, right deflections of a few hundred meters were observed. At an angle of fire of 76°, the shell experienced marginal deflections to the

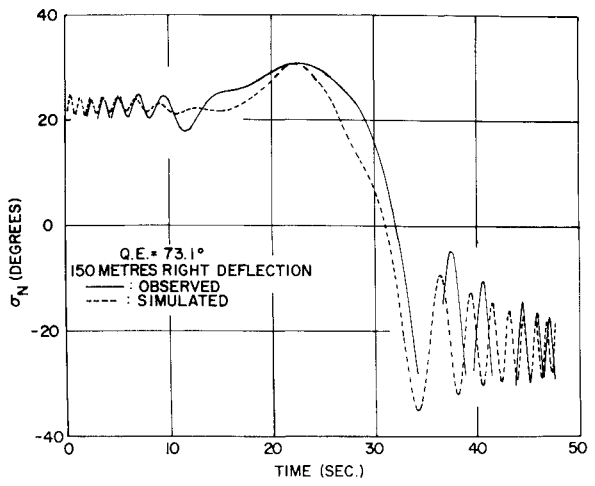

Fig. 4 Solar aspect angle history for round 5884.

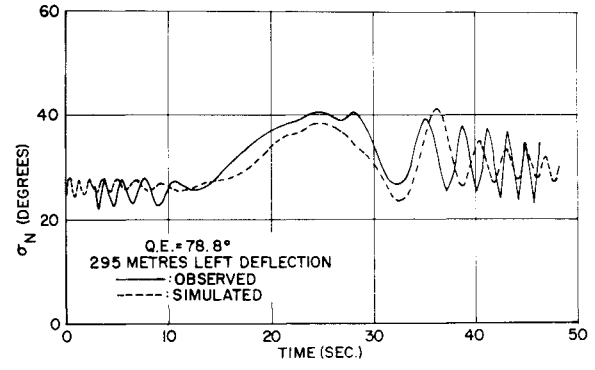

Fig. 5 Solar aspect angle history for round 5883.

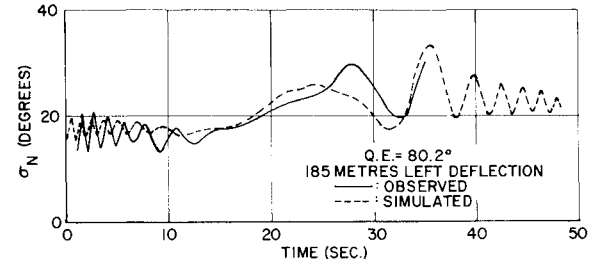

Fig. 6 Solar aspect angle history for round 5887.

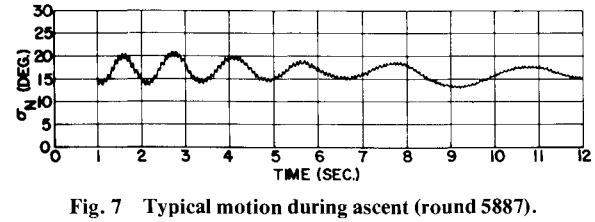

Fig. 7 Typical motion during ascent (round 5887).

left of the line of fire. The launch angle of 76°, therefore, represents the onset of left deflection for the 105-mm *M1* shell fired at a nominal muzzle velocity of 250 m/sec.

Above 76°, drift reversal was very pronounced—left deflections of several hundred meters were observed. There was some spread in the magnitude of the left deflections and this was due to variations in wind conditions aloft. In general, however, all shell were subjected to cross winds. It is confirmed, therefore, that artillery shell do drift to the left when fired under the proper "mix" of launch velocity and launch angle.

Now consider the three yawsonde flights. Figures 4-6 are plots of solar aspect angle vs time of flight for rounds 5884, 5883, and 5887, respectively. Also shown on Figs. 4-6 are the respective launch elevations and deflections as determined by the particular radar track. The time scale was chosen to show the overall characteristics of the motion. The data dropouts for rounds 5884 and 5887 are due to the amplitude of the motion exceeding the measurement range of the sun sensors. The solid curves are the measured yawsonde data. The dashed curves are the results of simulating these flights and will be discussed later (see Sec. VI).

To show the fine details of the motion and the resolution that is obtained by the yawsonde technique, the first few seconds of data for round 5887 is presented in Fig. 7. This early motion is typical of all yawsonde flights.

Since the motion of the three yawsonde flights during ascent are dynamically similar, only round 5887 will be discussed (Figs. 6 and 7). The first 15 sec or so of flight are characterized by small amplitude epicyclic motion, i.e., nutational and precessional motion. The fast frequency is associated with the nutational arm and the slow frequency with the precessional arm. The nutational frequency is constant at about 12 Hz and the nutational amplitudes decreases from about 1.5° to 0.5° (amplitudes are peak-to-peak values). The amplitude of the precessional motion is damped from about 6° to 3° with the frequency decreasing from 1 to about 0.25 Hz. At about 15 sec the precessional motion is essentially damped out. The aspect angle then increases as the shell approaches apogee, which occurs at 22.9 sec. Recalling that the azimuthal planes of the sun and gun are perpendicular to each other, the increase in aspect angle over this segment of the flight means that the nose is turning into the sun, i.e., the nose is turning to the right of the flight path. This is the yaw of repose effect. Near apogee the projectiles trim at fairly constant angles of attack and remain so until sometime after apogee.

Attention is now directed to the character of the motion during descent. Consider the first yawsonde flight, round 5884, Fig. 4. This projectile was fired at 73.1° which is the lowest angle of fire of the three yawsonde rounds, and one for which right deflection was expected. A right deflection of about 150 m was observed. At 22.3 sec the shell reached apogee and began its descent. The aspect angle is positive but soon starts to decrease. At about 32 sec, the aspect angle crosses zero° and continues through negative values over the remainder of the flight. The significance of the change in sign of aspect angle is illustrated in Fig. 8. During ascent the aspect angle is positive, which means that the sun's rays are incident on the shell from the direction of the nose. When the aspect angle is zero degrees, the solar vector is perpendicular to the longitudinal axis of the shell. Negative aspect angles mean the solar vector is between the normal and the base of the shell. Round 5884, therefore, turned over and flew nose forward during descent. (A shell is flying nose forward if the angle between the local tangent to the trajectory, i.e., the local velocity vector, and the longitudinal axis of the shell is less than 90°.) Ballisticians say such a projectile is "trailing its trajectory." Between 34 and 36 sec the shell begins large amplitude yawing motion, still nose forward, and continues this motion until impact. This motion is predominantly damped precession.

Now consider the second yawsonde flight, round 5883 (Fig. 5). Radar showed a left deflection of 295 m. Apogee occurred at 22.6 sec. Significantly, the aspect angle is not only positive on the up leg, but remains positive even during descent. The interpretation of this result is illustrated in Fig. 9. Since the aspect angle is positive over the entire flight, the solar vector is always between the normal and the nose. The only way this can occur on the down leg segment of the trajectory is for the shell to fly base forward. This means that round 5883 did not turn over after reaching the summit and was essentially flying backwards with its nose up and tail down. At 28 sec the shell begins large amplitude yawing motion. The nutational am-

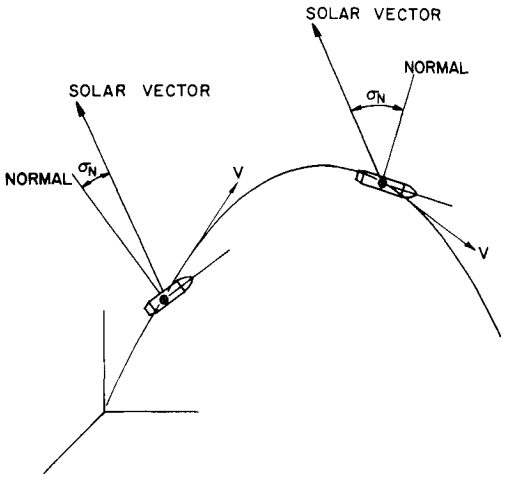

Fig. 8 Effect of trajectory curvature on aspect angle for trailing projectile (aspect angle is positive during ascent and negative during descent).

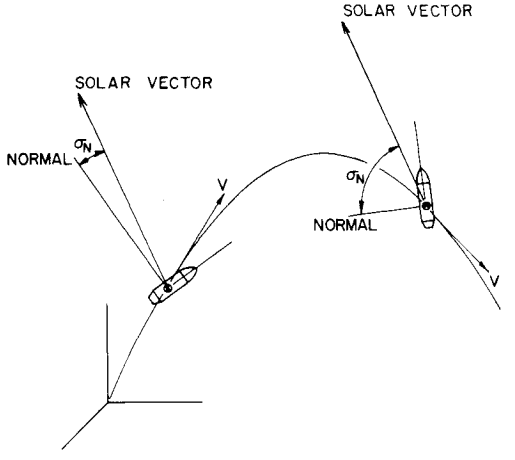

Fig. 9 Effect of trajectory curvature on aspect angle for nontrailing projectile (aspect angle is positive over entire trajectory).

plitude increases from 0° to approximately 3° at impact with the nutational frequency decreasing from about 12 to 10 Hz. The amplitude of the precessional motion is damped from about 14° to 9° with the frequency increasing from 0.14 to 0.33 Hz.

Now consider the last yawsonde flight, round 5887 (Fig. 6). The shell was fired at 80.2° and a left defelction of 185 m was observed. The amplitude of the motion during descent was intermittently greater than the measurement range of the sun sensors. It was decided not to reduce this section of the flight on the hybrid computer. However, a visual examination of the data pulses confirmed that the aspect angle was positive throughout the flight. Therefore, this shell also failed to turn over after reaching the summit and flew base forward during descent.

VI. Analysis

The method of Chapman and Kirk,[7] as programed by Whyte and Hathaway,[8] was used to determine the aerodynamic coefficients from the yawsonde data. This technique fits the equations of motion directly to the yawsonde data, with the coefficients as parameters of the fit. Data intervals of 6 sec were used in the fit. Due to computer memory limitations and the large amount of available data, every third data point within a given interval was used. The intervals started at the beginning of the data and moved along the data in one second increments. The static moment coefficient C_{M_α} damping moment coefficient $C_{M_q}+C_{M_{\dot\alpha}}$ and Magnus moment coefficient $C_{M_{p\alpha}}$ were assumed linear and computed over the portions of the trajectories in Table 1.

The coefficients obtained for these intervals are plotted against Mach number in Figs. 10, 11, and 12. It is emphasized that these Chapman-Kirk derived coefficients are from the early segments of the flights where epicyclic motion is dominant and yaw levels are small—generally less than 10°. Values of the coefficients used in the aspect angle simulations, to be discussed soon, are also shown on the respective graphs.

A possible source of difficulty is indicated in Fig. 13, which is a plot of Magnus moment coefficient vs damping moment coefficient. The figure shows that the coefficients are not independent, which may be due to the assumption that the coef-

Table 1 Coefficients computed over portions of trajectories

Round no.	Portion of trajectory
5884	1.64 to 12.64 sec
5883	3.22 to 13.22 sec
5887	1.20 to 8.20 sec

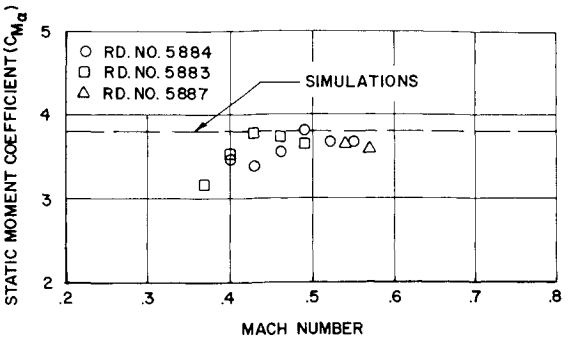

Fig. 10 Static moment coefficient vs Mach number.

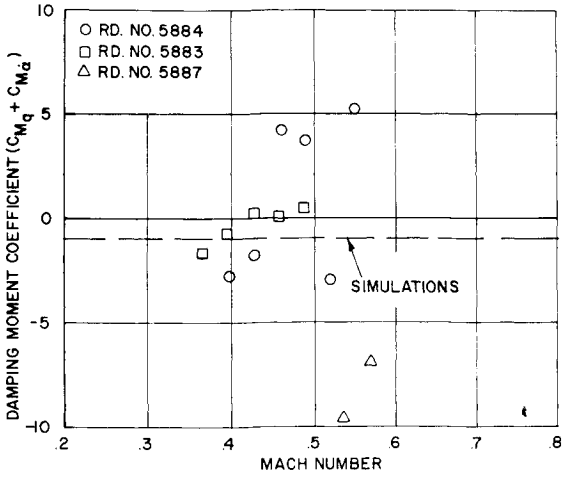

Fig. 11 Damping moment coefficient vs Mach number.

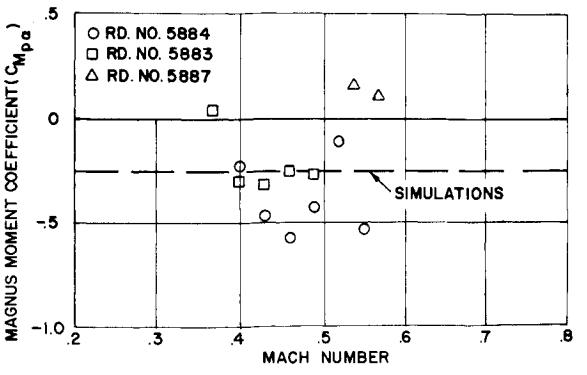

Fig. 12 Magnus moment coefficient vs Mach number.

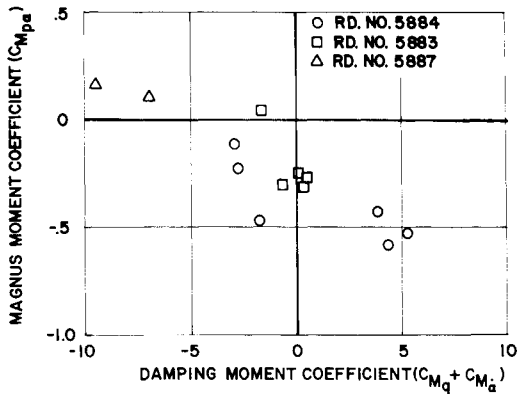

Fig. 13 Magnus moment coefficient vs damping moment coefficient.

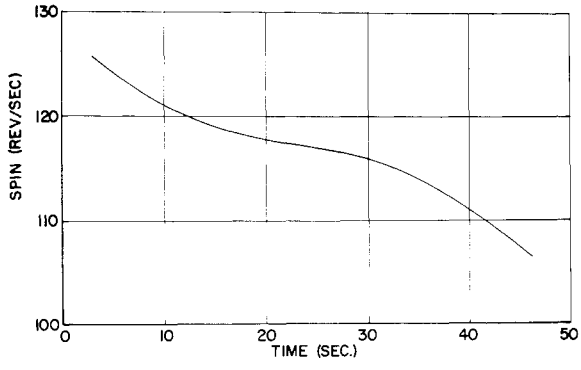

Fig. 14 Smoothed spin history for round 5883.

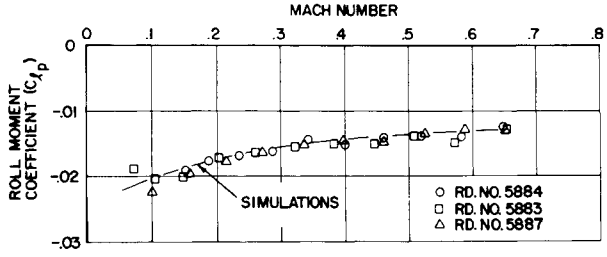

Fig. 15 Roll moment coefficient vs Mach number.

ficients are linear or may indicate that one or both of the yaw arms—nutation and precession—are poorly determined. This lack of independence implies that there is a need for an additional investigation into a more complete representation of the aerodynamic coefficients as functions of yaw.

A representative smoothed spin history is shown in Fig. 14. The local slope is the spin deceleration. The roll moment coefficient was determined from the spin deceleration and is plotted against Mach number in Fig. 15. The values of this coefficient used in the aspect angle simulations are also indicated.

The small yaw coefficients as determined by the method of Chapman-Kirk were coupled with large yaw coefficients from recent wind tunnel tests[9] and the six-degree-freedom (6DOF) trajectory model[10] was used to compute solar aspect angle histories for the yawsonde flights. Physical characterisitics of the rounds, gun position, and atmospheric conditions as recorded during the firing program were used in this simulation. The local yaw and trajectory were computed; and, from the known position of the sun, the local aspect angle was computed. The simulated and observed motions for a given flight were compared.

The simulated sun angle histories for rounds 5884, 5883, and 5887 are the dashed curves in Figs. 4-6, respectively. Overall, the computed angle histories compare favorably with observed data; all the features of the motion are present in the simulations—early damped epicyclic motion followed by a summital maneuver and damped precessional motion during descent. The 6DOF trajectory model simulates both nose first and base first descent. Early in the flights the frequencies of the nutational and precessional arms are similar; the major difference is greater damping of the precessional arm for the simulations than for the observed data. Except for slight phase discrepancies and differences in damping rates, the descending segments of the simulated and yawsonde flights are similar. The simulations are particularly sensitive to Magnus moment and damping moment coefficients and relatively insensitive to the roll moment coefficient.

VII. Discussion and Conclusions

The phenomenon of left drift has been confirmed. A quadrant elevation of 76° represents the onset of left deflection for the 105mm M1 shell fired at a nominal muzzle velocity of 250 m/sec— for quadrant elevations greater than 76°, the shell deflect to the left of the line of fire.

Interpretation of the yawsonde data shows that projectiles which deflect to the left are flying base forward during descent. After reaching the summit, such shell do not turn over and are flying at angles of attack greater than 90° with the base of the shell pointed toward the earth.

During ascent the three yawsonde flights experienced similar small amplitude yawing motion. At some point during descent, all three flights began to execute large amplitude yawing motion which persisted until impact. The significant difference is that the two higher angle of fire flights (78.8 and 80.2°) execute this motion in a base forward orientation. All flights experienced damped precessional motion during descent. There is stronger nutational motion for the two base forward rounds. Little, if any, down leg nutational motion is discernible for the flights which flew nose forward.

The Chapman-Kirk method, when applied to the small yaw portion of the data, produced estimates for the static, damping, and Magnus moment coefficients which were used, in conjunction with large yaw coefficients, to simulate the aspect angle histories for the yawsonde flights. The simulations match the observed yawsonde data quite well.

References

[1] Murphy, C. H., "Gravity-Induced Angular Motion of a Spinning Missile," *Journal of Spacecraft and Rockets,* Vol. 8, March 1971, pp. 259-263 (Also published as Ballistic Research Lab. Rept. 1546, AD 73041, July 71, Aberdeen Proving Ground, Md.).

[2] Collings, W. Z. and Lieske, R. F., "A Study of Artillery Shell Drift at High Angle of Fire Using Solar Aspect Sensors," BRL MR 2244, Nov. 1972, Ballistic Research Labs., Aberdeen Proving Ground, Md.

[3] Clay, W. H., "A Precision Yawsonde Calibration Technique," BRL MR 2263, Jan. 1973, Ballistic Research Labs., Aberdeen Proving Ground, Md.

[4] Mermagen, W. H., "Measurements of the Dynamical Behavior of Projectiles Over Long Flight Paths," *Journal of Spacecraft and Rockets,* Vol. 8, April 1971, pp. 380-385.

[5] Mermagen, W. H., "Miniature Telemetry Systems for Gun-Launched Instrumentation," *Proceedings of the Fourteenth International ISA Aerospace Instrumentation Symposium,* Instrument Society of America, Vol. 14, 1968, pp. 225-235.

[6] Collings, W. Z., "Reduction of Yawsonde Data on the EAI 690 Hybrid Computer," Aberdeen Proving Ground, Md., Ballistic Research Lab. BRL Rept. (to be published).

[7] Chapman, G. T. and Kirk, D. B., "A New Method for Extracting Aerodynamic Coefficients from Free Flight Data," *AIAA Journal,* Vol. 8, April 1970, pp. 753-758.

[8] Whyte, R. H. and Hathaway, W. H., "Reduction of Yawsonde and Position Time Radar Data by Numerical Integration," GE No. 72APB506, Jan. 1972, Armament Systems Dept., General Electric Co., Burlington, Vt.

[9] McCoy, R.L., "Subsonic Aerodynamic Characteristics of the 105mm HE Shell, M1 at Angles of Attack from Zero to 180 Degrees," BRL MR 2353, March 1974, Ballistic Research Labs., Aberdeen Proving Ground, Md.

[10] Lieske, R.F. and McCoy, R.L., "Equations of Motion of a Rigid Projectile," BRL R 1244, AD 441598, March 1964, Ballistic Research Labs., Aberdeen Proving Ground, Md.